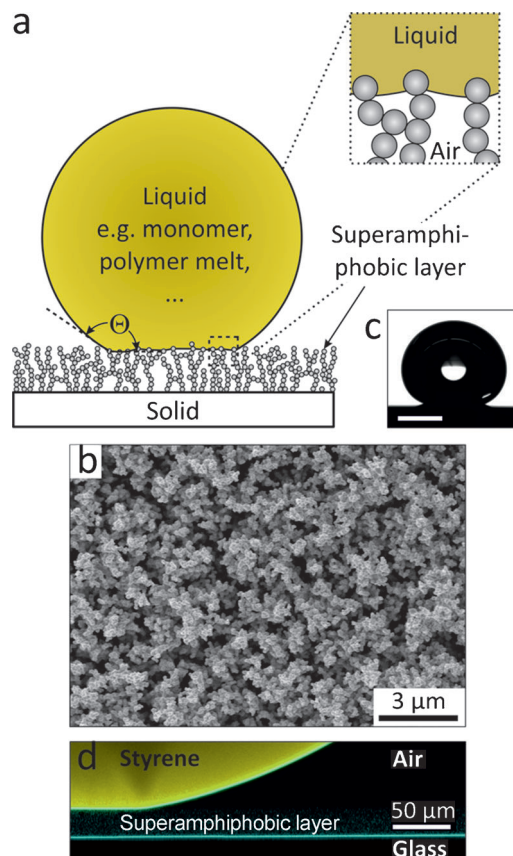


# Solvent-Free Synthesis of Microparticles on Superamphiphobic Surfaces\*\*

Xu Deng, Maxime Paven, Periklis Papadopoulos, Ming Ye, Si Wu, Thomas Schuster, Markus Klapper, Doris Vollmer,\* and Hans-Jürgen Butt\*

Polymer particles constitute a large part of synthetic materials. Multicomponent polymer-based microspheres find applications in drug delivery,<sup>[1]</sup> protein isolation and analysis,<sup>[2]</sup> photonics,<sup>[3]</sup> and displays.<sup>[4]</sup> Depending on the function, different materials, sizes, and structures are required, including microgels,<sup>[1b]</sup> core-shell, patchy, multicompartment, and Janus particles.<sup>[4b,5]</sup> Most well-known strategies for the synthesis of particles include dispersion, emulsion, and mini-emulsion polymerization.<sup>[6]</sup> Microparticles are produced in solution or in a confinement formed of immiscible solvents and emulsifiers. Multicomponent, functional microparticles<sup>[5a,c,e,7]</sup> can also be synthesized by modern techniques, for example, by microfluidic, photo,<sup>[3b,5b,8]</sup> or thermal polymerization,<sup>[4b]</sup> or by evaporation of water from a dispersion.<sup>[9]</sup> All these methods rely on solvents or processing liquids and often involve the use of surfactants. For environmental reasons and to reduce energy consumption, it is desirable to develop strategies that reduce or completely avoid any type of solvent or emulsifier.

Here we show that polymeric and composite microspheres can be produced without solvents, process liquids, or additives by using superamphiphobic layers. Superamphiphobic layers extend the water repellency of superhydrophobic surfaces to organic liquids and aqueous solutions of surfactants or proteins.<sup>[10]</sup> On superamphiphobic layers, even nonpolar liquids form an apparent contact angle above 150° and a roll-off angle below 10° in air (Figure 1a). For superamphiphobicity, low interfacial energy and microscopic protrusions with overhanging geometries are essential.<sup>[10d,11]</sup> Microscopic pockets of air are trapped beneath the liquid. The drop rests on top of the protrusions, and the interfacial tension of the liquid causes the drop to assume a spherical shape, much like a freely suspended or falling drop (see the Supporting Information). Furthermore, because the real solid-liquid interfacial area is much smaller than the apparent



**Figure 1.** Liquid drop on a superamphiphobic layer. a) Schematic of a liquid drop on a superamphiphobic layer and a magnified view of the interface between the liquid and the superamphiphobic layer. b) SEM image of a superamphiphobic layer. c) Video image and d) vertical section of a drop of styrene on a superamphiphobic layer imaged with a confocal microscope (contact angle  $\Theta = 158^\circ$ , roll-off angle  $\alpha = 6^\circ$ ). Scale bar in (c): 1 mm. The 6  $\mu\text{L}$  drop was labeled with *N*-(2,6-diisopropylphenyl)perylene-3,4-dicarboxylic acidimide (0.04  $\text{mg mL}^{-1}$ ) and thus appeared yellow. The reflection of the excitation light (cyan) at the interfaces shows the top surface of the glass and the bottom surface of the styrene drop. In between, with some weak scattering at the silicon oxide nanostructures the superamphiphobic layer can be seen.

[\*] Dr. X. Deng, M. Paven, Dr. P. Papadopoulos, Dr. M. Ye, Dr. S. Wu, T. Schuster, Dr. M. Klapper, Dr. D. Vollmer, Prof. Dr. H.-J. Butt  
Max Planck Institute for Polymer Research  
Ackermannweg 10, 55128 Mainz (Germany)  
E-mail: vollmerd@mpip-mainz.mpg.de  
butt@mpip-mainz.mpg.de  
Homepage: <http://www.mpip-mainz.mpg.de>

[\*\*] The authors are grateful to A. Kaltbeitzel and G. Glasser for their technical support. Financial support is gratefully acknowledged from SPP 1420 (H.J.B.), SPP 8173 (D.V.), SPP 8203 (X.D.), and SFB-TR6 (P.P.).



Supporting information for this article is available on the WWW under <http://dx.doi.org/10.1002/anie.201302903>.

contact area, adhesion of the drop to the surface is low, leading to a low roll-off angle.<sup>[11b]</sup>

The proposed method to fabricate polymeric microspheres takes advantage of the high liquid repellency of superamphiphobic layers. The almost spherical shape of the drops and the extremely low adhesion of the particles to the layer allow polymeric microspheres to be synthesized on superamphiphobic layers, as demonstrated for a radical

polymerization. Janus and magnetic microspheres are produced by melting agglomerates of polymeric powders. The polymerized or solidified solid microspheres can be easily removed from the superamphiphobic layer without leaving polymer behind or changing the topography of the layer.

We recently developed a simple method to fabricate optically transparent, robust superamphiphobic layers (Figure 1).<sup>[12]</sup> Our design is based on a fractal-like arrangement of nanoparticles. A template of soot particles (30–50 nm in diameter) is coated with a 20–30 nm thick layer of SiO<sub>2</sub> (Figure 1b). To render the layer transparent, the soot is burned away at 600 °C. Finally, the porous SiO<sub>2</sub> layer is coated with (tridecafluoro-1,1,2,2-tetrahydrooctyl)-1-trichlorosilane to lower the surface energy (Figure 1c,d). The layer is UV resistant, stable up to 400 °C, optically transparent, and does not swell in organic or polar liquids. This opens up the opportunity to fabricate almost contact-free solid–liquid interfaces.

The repellency of our superamphiphobic layers is demonstrated for styrene (Figure 1d). In the confocal-microscope image, the fluorescently labeled drop of styrene remains on top of the superamphiphobic layer without impaling it. The vertical cross-section also shows the high contact angle. A similarly high contact angle was observed for several other monomers (Table 1).

**Table 1:** Contact angle  $\theta$ , roll-off angle  $\alpha$ , and surface tension  $\gamma$  of some monomers on a superamphiphobic surface at 20 °C. Drop volume:  $(6 \pm 1) \mu\text{L}$ . The surface tensions were measured by using the Wilhelmy-plate method.

Monomer	$\theta$	$\alpha$	$\gamma$ [mN m <sup>-1</sup> ]
styrene	158°	6°	34
methyl methacrylate	156°	10°	28
acrylic acid	154°	7°	29
adipoyl chloride	152°	9°	38
ethylenediamine	152°	16°	42

To demonstrate that superamphiphobic layers can be used for solvent-free polymerization of microparticles, we carried out a radical polymerization of a methacrylate initiated by UV light. We mixed bisphenol A glycerolate dimethacrylate (bis-GMA) and tri(ethylene glycol) dimethacrylate (TEGDMA) with the photoinitiator phenylbis(2,4,6-trimethylbenzoyl)phosphine oxide. A drop of the mixture was placed with a pipette on a slightly concave watch glass coated with a superamphiphobic layer (Figure 2a). The mixture showed a static contact angle of 159° and a roll-off angle of 20°. Polymerization was initiated by UV irradiation. To avoid deformation because of gravity or adhesion, the watch glass was moved by a 2D orbital shaker to keep the drop in rolling motion while its viscosity continuously increased. The polymerized particles rolled off from the superamphiphobic layer when the substrate was tilted by a few degrees. The adhesion to particles is extremely low because actual contact is only established at few points. To produce small particles, we deposited the mixture by an inkjet printer. Particle diameters of only a few 10  $\mu\text{m}$  were obtained (Figure 2d).

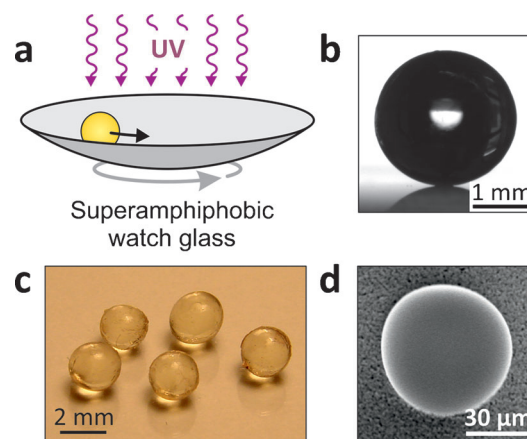


**Figure 2.** Synthesis of microspheres by radical polymerization. a) Schematic of the set-up. b,c) Particles synthesized from bis-GMA (15 wt%), TEGDMA (84 wt%), and photoinitiator (1 wt%). After mixing and sonication for 30 min, a drop (8–10  $\mu\text{L}$ ) was pipetted into a concave watch glass (10 cm diameter, 1.5 cm high) coated with a superamphiphobic layer. The polymerization was initiated by pulsed UV irradiation for 1 min followed by continuous illumination for 4 min (LQ 400, UV-A: 200 mWcm<sup>-2</sup> at the end of the glass fiber). d) SEM image of a microsphere from 99 wt% TEGDMA with 1 wt% photoinitiator polymerized by UV exposure for 3 min. The mixture was deposited by an inkjet printer (Nano-Tip JA 070-401) held at a distance of 4 cm.

The size of the spherical particles corresponds to the initial volume of the monomer drop. The degree of monodispersity is given by the accuracy of depositing drops of a well-defined volume. We are able to synthesize particles as large as a few millimeters (Figure 2b,c). The upper limit is determined by the effect of gravity, which for drops larger than the capillary length flattens the drops. The capillary length is  $\kappa = \sqrt{\gamma/g\rho}$  with the surface tension  $\gamma$ , the density  $\rho$ , and  $g = 9.81 \text{ m s}^{-2}$ . Typically,  $\kappa$  is about 2 mm. The fundamental lower limit is given by the spacing between neighboring protrusions. Particles smaller than the spacing between protrusions penetrate the superamphiphobic layer. For these superamphiphobic layers, this spacing was about 1  $\mu\text{m}$ .

It is essential to keep the drops rolling during polymerization, otherwise the particles may adhere to the surface and form a planar area at the contact region. To demonstrate this effect, we heated polystyrene powder above its glass transition. The powder particles formed spheres because of the surface tension of the polystyrene. After cooling, flat regions were observed where the particle was in contact with the superamphiphobic layer (Figure 3a). These flat regions were also observed after removing the particles from the superamphiphobic layer (Figure 3b). However, keeping the superamphiphobic surface in motion during solidification leads to defect-free spherical particles (Figure 3c). We verified by scanning electron microscopy (SEM) that the particle synthesis does not damage the superamphiphobic layer. This can be understood considering that the applied forces are extremely weak.

As the superamphiphobic layers remain stable up to 400 °C, microspheres can also be produced by heating

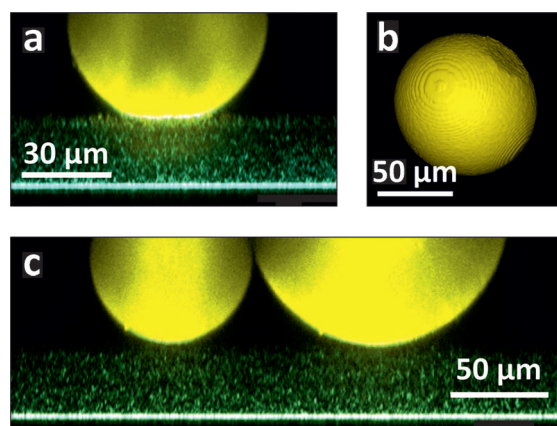


**Figure 3.** Confocal images of polystyrene particles formed on a superamphiphobic layer after heating the powder to 100 °C. a) Vertical cross-section. b) Particle showing the previous contact area on the top right side. c) Two polystyrene particles without a flat area. Polystyrene was labeled with rhodamine B ( $M_w = 13.8 \text{ kg mol}^{-1}$ ,  $T_g = 91 \text{ °C}$ ; synthesis described in the Supporting Information).

a thermoplastic polymer powder or blend above its glass-transition temperature ( $T_g$ ; Figure 4a). As an example, we fabricated polystyrene microspheres (see Supporting Movie S1, and Figure S1 in the Supporting Information) and magnetic hybrid microspheres. Microparticles with a permanent magnetic dipole moment are useful as microrheological probes and magnetic micromixers,<sup>[8b,c]</sup> and they are used in various biomedical applications, for example, in immunoassays and for protein analysis.<sup>[2,8b]</sup> Polystyrene was mixed with iron oxide nanoparticles (Figure S2 in the Supporting Information) and deposited on a superamphiphobic layer (Figure 4b). The powder agglomerate was heated at 165 °C for 2 h while a magnetic field of 35 mT was simultaneously applied to orient the iron oxide nanoparticles. The spherical shape and the orientation of the nanoparticles were preserved after cooling.

To demonstrate that the composite microspheres acquired a permanent magnetic dipole moment, we dispersed individual microspheres in water and exposed them to a weak, rotating magnetic field (Figure 4c,d). The microspheres rotated with a frequency corresponding to the external magnetic field (Figure S3 in the Supporting Information). When the polymer melt solidified without applying an external field, the microspheres did not rotate but performed an oscillatory or rocking motion (Figure 4d and Supporting Movie S2). Cryo-focused ion beam milling combined with SEM showed that the nanoparticles formed elongated aggregates when an external magnetic field was applied during heating (Figure S4 in the Supporting Information).

To document the generality of our synthetic approach, we also exploited the high liquid repellency of superamphiphobic layers to produce Janus microspheres from polystyrene and poly(methyl methacrylate) (PMMA). The polystyrene/PMMA blend (synthesis described in the Supporting Information) was placed on a superamphiphobic layer and annealed at 160 °C. This temperature was well above the glass-transition temperatures of both polystyrene ( $T_g = 91 \text{ °C}$ ) and PMMA ( $T_g = 120 \text{ °C}$ ). Polystyrene was tacked with

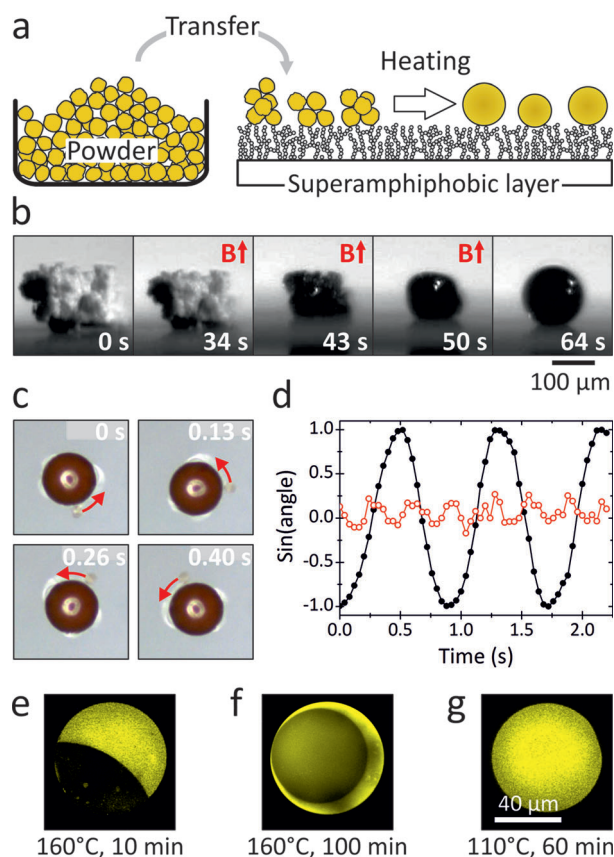


**Figure 4.** Microspheres produced by melting a thermoplastic polymer on a superamphiphobic layer. a) Schematic of the strategy. b) Sequence of video microscope images of a polystyrene/iron oxide composite powder annealed at 165 °C for 2 h in a magnetic field of 35 mT ( $B \uparrow$ ) on a superamphiphobic layer. Polystyrene was synthesized in house by anionic polymerization ( $M_w = 5.8 \text{ kg mol}^{-1}$ ,  $T_g = 78 \text{ °C}$ ). The composite microsphere contained 12 vol% of iron oxide. c) Video microscope images of a polystyrene/iron oxide microsphere in water, rotating in an external magnetic field of 1.3 mT at 1.2 Hz. The rotation can be seen following the defect indicated by the red arrow. d) Sine of the orientation of a composite microsphere fabricated in the presence (black) and absence (red) of an external magnetic field. e–g) SEM images of a particle of a polystyrene/PMMA blend annealed e) at 160 °C for 10 min, f) at 160 °C for 100 min, and g) at 110 °C for 1 h. Polystyrene was labeled with rhodamine B. Excitation wavelength: 570 nm.

a fluorescent dye to visualize the phase separation by confocal microscopy. As we used a blend containing equal amounts of polystyrene and PMMA (1:1 *w/w*), the Janus microspheres also consisted of polystyrene and PMMA in a *w/w* ratio of 1:1 (Figure 4e). The degree of phase separation depends on the annealing period and particle size (Figure S5 in the Supporting Information). As polystyrene shows a lower interfacial tension with air than with PMMA, polystyrene in thermodynamic equilibrium embeds PMMA.<sup>[13]</sup> This was indeed observed when annealing for a long time (100 min at 160 °C in Figure 4f). Thus, the surface properties can be tuned by the duration of annealing. To verify that phase separation requires the heating of both components above their glass-transition temperatures, we annealed another particle at 110 °C for 1 h (Figure 4g). No phase separation was observed.



In conclusion, superamphiphobic layers can be used for solvent- and emulsifier-free particle synthesis. Particles can be prepared by polymerization or by melting a single polymer without surface-active compounds. The particles can be removed easily from the superamphiphobic layer. Therefore, the presented approach complements previous work in which (nano)particles were prepared on top of superhydrophobic pillars.<sup>[14]</sup> These (nano)particles adhered to the surface of the pillar. Avoiding solvents excludes the pollution of a continuous phase by monomers, initiators, etc. Expensive purification of a continuous aqueous phase, which is a problem in industrial emulsion polymerization, can be avoided. Furthermore, migration and ageing effects that result from a slow phase separation between particles and stabilizers, typically occurring in particle films, are avoided. Finally, this method opens the door to a new generation of particles for medical applications. The main limitation of the presented approach is the throughput, which resembles those achievable by microfluidics (typical particle producing rate: 100–1000 particles per second). The throughput of this method is dominated by the time it takes to deposit liquid drops (the speed of droplet generation can reach up to 100 drops per second with an inkjet printer) or powders on the surface, the polymerization rate, and the time required to melt a polymer powder, to orient magnetic nanoparticles, or to phase-separate polymer blends.

Received: April 8, 2013

Revised: June 13, 2013

Published online: September 5, 2013

**Keywords:** Janus particle · magnetic particles · microspheres · polymerization · superamphiphobic surfaces

- [1] a) A. C. Lima, P. Sher, J. F. Mano, *Expert Opin. Drug Delivery* **2012**, 9, 231; b) S. H. Ma, J. Thiele, X. Liu, Y. P. Bai, C. Abell, W. T. S. Huck, *Small* **2012**, 8, 2356.
- [2] J. W. Choi, K. W. Oh, J. H. Thomas, W. R. Heineman, H. B. Halsall, J. H. Nevin, A. J. Helmicki, H. T. Henderson, C. H. Ahn, *Lab Chip* **2002**, 2, 27.
- [3] a) J. F. Galisteo-López, M. Ibasate, R. Sapienza, L. S. Froufe-Pérez, A. Blanco, C. López, *Adv. Mater.* **2011**, 23, 30; b) D. Dendukuri, P. S. Doyle, *Adv. Mater.* **2009**, 21, 4071.
- [4] a) B. Comiskey, J. D. Albert, H. Yoshizawa, J. Jacobson, *Nature* **1998**, 394, 253; b) T. Nisisako, T. Torii, T. Takahashi, Y. Takizawa, *Adv. Mater.* **2006**, 18, 1152; c) A. Ghosh, N. K. Sheridan, P. Fischer, *Small* **2008**, 4, 1956.
- [5] a) K. H. Roh, D. C. Martin, J. Lahann, *Nat. Mater.* **2005**, 4, 759; b) Z. H. Nie, W. Li, M. Seo, S. Q. Xu, E. Kumacheva, *J. Am. Chem. Soc.* **2006**, 128, 9408; c) J. Z. Du, R. K. O'Reilly, *Chem. Soc. Rev.* **2011**, 40, 2402; d) Q. Chen, J. K. Whitmer, S. Jiang, S. C. Bae, E. Luijten, S. Granick, *Science* **2011**, 331, 199; e) J. Hu, S. X. Zhou, Y. Y. Sun, X. S. Fang, L. M. Wu, *Chem. Soc. Rev.* **2012**, 41, 4356.
- [6] K. Matyjaszewski, T. P. Davis, *Handbook of Radical Polymerization*, Wiley, Hoboken, **2002**.
- [7] J. J. Kaufman, G. M. Tao, S. Shabahang, E. H. Banaei, D. S. S. Deng, X. D. Liang, S. G. Johnson, Y. Fink, A. F. Abouraddy, *Nature* **2012**, 487, 463.
- [8] a) S. Q. Xu, Z. H. Nie, M. Seo, P. Lewis, E. Kumacheva, H. A. Stone, P. Garstecki, D. B. Weibel, I. Gitlin, G. M. Whitesides, *Angew. Chem.* **2005**, 117, 734; *Angew. Chem. Int. Ed.* **2005**, 44, 724; b) C. H. Chen, A. R. Abate, D. Y. Lee, E. M. Terentjev, D. A. Weitz, *Adv. Mater.* **2009**, 21, 3201; c) K. P. Yuet, D. K. Hwang, R. Haghgoie, P. S. Doyle, *Langmuir* **2010**, 26, 4281.
- [9] a) V. Rastogi, S. Melle, O. G. Calderón, A. A. García, M. Marquez, O. D. Velev, *Adv. Mater.* **2008**, 20, 4263; b) A. G. Marín, H. Gelderblom, A. Susarrey-Arce, A. van Houselt, L. Lefferts, J. G. E. Gardeniers, D. Lohse, J. H. Snoeijer, *Proc. Natl. Acad. Sci. USA* **2012**, 109, 16455.
- [10] a) S. Shibuichi, T. Yamamoto, T. Onda, K. Tsujii, *J. Colloid Interface Sci.* **1998**, 208, 287; b) W. Chen, A. Y. Fadeev, M. C. Hsieh, D. Öner, J. Youngblood, T. J. McCarthy, *Langmuir* **1999**, 15, 3395; c) Q. D. Xie, J. Xu, L. Feng, L. Jiang, W. H. Tang, X. D. Luo, C. C. Han, *Adv. Mater.* **2004**, 16, 302; d) A. Tuteja, W. Choi, M. L. Ma, J. M. Mabry, S. A. Mazzella, G. C. Rutledge, G. H. McKinley, R. E. Cohen, *Science* **2007**, 318, 1618; e) X. Yao, Y. L. Song, L. Jiang, *Adv. Mater.* **2011**, 23, 719; f) S. Pan, A. K. Kota, J. M. Mabry, A. Tuteja, *J. Am. Chem. Soc.* **2013**, 135, 578.
- [11] a) S. Herminghaus, *Europhys. Lett.* **2000**, 52, 165; b) H. J. Butt, C. Semperebon, P. Papadopoulos, D. Vollmer, M. Brinkmann, M. Ciccotti, *Soft Matter* **2013**, 9, 418.
- [12] X. Deng, L. Mammen, H.-J. Butt, D. Vollmer, *Science* **2012**, 335, 67.
- [13] D. Marenduzzo, E. Orlandini, *Soft Matter* **2013**, 9, 1178.
- [14] a) B. D. Hatton, J. Aizenberg, *Nano Lett.* **2012**, 12, 4551; b) J. W. Krumpfer, T. J. McCarthy, *J. Am. Chem. Soc.* **2011**, 133, 5764; c) R. Dufour, P. Brunet, M. Harnois, R. Boukherroub, V. Thomy, V. Senez, *Small* **2012**, 8, 1229; d) B. Su, S. Wang, J. Ma, Y. Song, L. Jiang, *Adv. Funct. Mater.* **2011**, 21, 3297; e) J. W. Krumpfer, P. Bian, P. Zheng, L. Gao, T. J. McCarthy, *Langmuir* **2011**, 27, 2166.